



## **EFFECT OF NON-LINEAR FLUID VISCOUS DAMPERS ON THE SIZE OF EXPANSION JOINTS OF MULTI-SPAN PRESTRESSED CONCRETE SEGMENTAL BOX-GIRDER BRIDGES**

**Stefano BERTON<sup>1</sup>, Hans STRANDGAARD<sup>2</sup> and John E. BOLANDER<sup>3</sup>,**

### **SUMMARY**

Modular expansion joints are important components of any long- or medium-span bridge. They are designed to provide continuity of the bridge deck where breaks in the superstructure are made to accommodate short- and long-term deformations of the bridge. Such deformations include thermal expansions, drying shrinkage, creep and, for structures located in active seismic regions, earthquake induced deformations. This paper presents the results of a numerical study to investigate the possibility of reducing, through the use of non-linear Fluid Viscous Dampers (FVDs), the size of the modular expansion joints of a multi-span segmental prestressed concrete bridge. For the case studied, the results show that by using non-linear FVDs, the expansion joints can be reduced up to 50% with respect to the original design size. This study also shows that by using FVDs the overall dynamic behavior of the model is improved reducing the risk of damage of the expansion joints due to possible pounding between bridge frames. Additional benefits include a significant reduction in the longitudinal pier moments.

### **INTRODUCTION**

Bridge deck expansion joints are important components of any bridge structure. In addition to accommodating the time-dependent deformations, expansion joints are designed to withstand traffic loading and to provide a smooth riding transition for the vehicular flow. Furthermore, expansion joints need to be resistant to environmental loadings and at the same time must prevent water and dissolved substances (e.g. deicing chemicals) from penetrating into the bridge structural components (Roeder [1]). Bridge deck expansion joints can be of many different types. For small and medium joint gaps (up to 25-150 mm) the expansion joint can be constructed by simply pouring special rapid-curing materials (e.g. silicone based materials) inside the preformed joint opening or by using neoprene type joints such as compression or strip seals (Chang [2]). For more important structures and when the expected relative movement of the joints exceeds 100 mm, modular expansion joints (or joint seal assemblies) are generally used. The basic system for this type of joint consists of a sliding grid of beams supported by longitudinal

---

<sup>1</sup> Post Doc. Researcher, Dept. Civil Engng., Kyushu University, Fukuoka 812-8581, Japan

<sup>2</sup> Senior Bridge Engr., CH2M HILL, 2485 Natomas Park Dr., Suite 600, Sacramento, CA 95833 USA

<sup>3</sup> Assoc. Professor, Dept. Civil & Environmental Engng., Univ. of California, Davis, CA 95616 USA

joists so that the joint opening is subdivided into smaller gaps. In general, this kind of joint can accommodate movements of up to 1500 mm.

Because joints are physical cuts of the bridge superstructure, pounding between the adjacent frames and intermediate joint unseating can occur during seismic events. These kinds of collapse and damage have been observed in many bridge structures during recent earthquakes. For this reason and for a better understanding of the phenomena, the dynamics of pounding between bridge frames and other civil structure components has been the object of several recent theoretical and experimental studies (Malhotra [3], Chau [4]). These studies show that the dynamic behavior of adjacent structures depends on several parameters, including the frame period ratio, the relative distance between frames (e.g. joint gap) and the characteristics of the input ground motion. To prevent joint (or hinge) unseating, the conventional approach consists of providing long seat lengths and linking the contiguous frames by seismic cable (or rod) restrainers. Several studies and restrainer design procedures have been proposed in the literature (Trochalachis [5], DesRoches [6]). However, current restrainer design guidelines are based on elastic criteria, although during major earthquakes the restrainers and their anchorages are likely to sustain severe plastic deformations (Feng [8]). Furthermore, restrainer systems in general do not provide any significant amount of energy dissipation during a seismic event. For these reasons, in recent major earthquakes, a number of bridges that were retrofitted or designed using seismic cable restrainers collapsed due to the failure of the restrainers or their anchorages (Moehle [7]).

Previous numerical studies have shown that the dynamic behavior of bridges can be improved by installing supplemental damping devices at the joint locations (Feng [8], Strandgaard [9]). In particular, dissipation devices can be used to reduce the risk of unseating at intermediate joints and also prevent damage due to possible pounding between contiguous frames. In this paper, the effects of supplemental damping devices on the dynamic behavior of bridge deck joints is investigated through a numerical example with particular focus on the reduction of the expansion joint size. The devices used in the simulations are non-linear fluid viscous dampers (FVDs). These devices are able to dissipate a considerable amount of energy and consequently reduce the relative seismic displacements and velocities at the bridge joint locations. Firstly, numerical simulations of the model without dampers are carried out for different sets of input ground motions. In the second phase, a method for estimating appropriate sizes of non-linear dampers is presented. Thereafter, a series of simulations is carried out using the model with such dissipation devices. The results are discussed and compared with those of the model without dampers.

## **NUMERICAL MODEL AND INPUT GROUND MOTIONS**

To investigate the effect of supplemental damping devices on the size of bridge deck expansion joints, an available finite element model of a prestressed concrete segmental box-girder bridge is used. The bridge is composed of a main structure (four main frames) and three approaches (three north approaches). Because of the size of the structure (the total superstructure length of the four main frames is about 2265 m), and the large movement that needs to be accommodated at the joint locations, modular expansion joints need to be used. The numerical model of the main structure and approaches is shown in Fig. 1. The model is composed of 723 three-dimensional beam elements for a total of 4198 degrees of freedom.

Three different sets of acceleration ground motions are used to carry out the nonlinear time history analyses (NLTH). Each set includes 3 components of acceleration: longitudinal, transverse, and vertical. Each set is different in terms of duration, peak acceleration and frequency components. For example, the duration of set #1 is 42 seconds while those of sets #2 and #3 are 40 and 21 seconds, respectively. In each NLTH analysis all three components are applied to the structure simultaneously. Two different levels of

ground motion intensity have been considered: a Safety Level Earthquake Event (SEE) and a Functional Level Earthquake Event (FEE). The SEE corresponds to an event with a 1,000 to 2,000 year return period based on a probabilistic design approach. The FEE event has been defined as a 300-year return period and an intensity, which corresponds to 65% of the SEE event. CH2M HILL provided the input ground motions and the numerical model used in this study. The non-linear version of the commercial finite element code SAP2000n (Wilson [10]) is used to carry out all the linear and non-linear analyses.

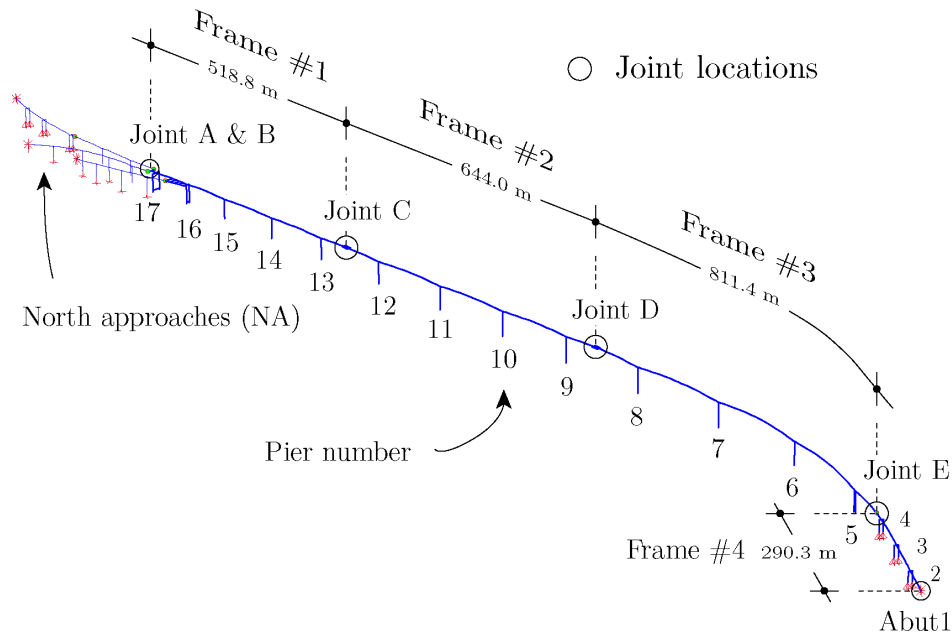


**Figure 1:** Finite element model of the bridge structure.

### EXPANSION JOINT DESIGN CRITERIA

The primary functions of expansion joints are to provide a watertight connection and to accommodate short- and long-term relative movements of the bridge components. Because of their continuous exposure to mechanical and environmental loading, joint seal maintenance is one of the most costly maintenance issues on bridges. Replacement of failed joints is also very expensive, yet many Departments of Transportation still try to minimize the initial costs of the joints they install. The cost of the joint is function of its movement rating, MR, defined as the maximum opening movement that the joint can accommodate. If the structure is important and located in an active seismic area, in general, the earthquake-induced movements should also be included by the specific-project design criteria as a component of the joint movement rating, MR. However, including all the deformation components simultaneously may result in excessive joint dimensions. For example, there is a small probability of a major earthquake occurring at the same time as the maximum temperature-induced deformation. Therefore, the criteria used in this study for the expansion joint MR calculation is as follows

$$MR = 1.5 \Delta_{CS}^{10} + \Delta_{FEE} \quad (1)$$

where  $\Delta_{CS}^{10}$  is the sum of the effects of creep and shrinkage developed during the 10 years after the installation of the expansion joints, and  $\Delta_{FEE}$  is the seismic excursion of the joint, defined as the sum of opening and closing relative movements of the joint faces due to the functional level earthquake loading. As previously pointed out, because of the small probability of the simultaneous occurrence of a major earthquake and the maximum temperature-induced deformation, this last effect is not included in the

calculation of the joint MR (Equation 1). Note however, that the temperature-induced deformation can be absorbed by a portion of the  $\Delta_{FEE}$  component during the normal operational time of the structure.

### TIME HISTORY ANALYSIS (WITHOUT DAMPERS)

An important component of the expansion joint movement rating, MR, is the seismic excursion  $\Delta_{FEE}$ . To calculate these values, a series of time history analyses of the bridge are carried out using the input ground motions previously described. The results in terms of maximum opening and minimum closing for the SEE are shown in Table 1. Note that only the values of Joints A through E and Abutment 1 are shown in the table. Although the numerical model includes the three north approaches, the installation of the dampers will be limited to the main frames. For this reason, the displacement results at the joint locations relative to the north approaches are not shown.

Joint	Ground motion #1			Ground motion #2			Ground motion #3		
	max open.	min closing	$\Delta_{SEE}$	max open.	min closing	$\Delta_{SEE}$	max open.	min closing	$\Delta_{SEE}$
A	49.1	-45.9	<b>95.0</b>	47.9	-46.6	94.5	44.0	-44.0	88.1
B	52.7	-49.4	102.1	46.2	-47.1	93.3	60.2	-57.6	<b>117.9</b>
C	45.6	-45.2	90.8	51.6	-50.7	<b>102.3</b>	43.9	-47.5	91.4
D	11.5	-10.3	21.8	15.2	-15.5	30.6	16.5	-17.0	<b>33.6</b>
E	62.5	-52.9	<b>115.5</b>	54.9	-55.8	110.7	54.7	-54.3	109.0
Abut. 1	34.8	-32.2	70.6	39.4	-38.5	<b>77.9</b>	37.6	-37.6	73.7

All values are expressed in centimeters

**Table 1:** Opening and closing displacements at joint and abutment locations for the model without dampers subjected to three input ground motions at SEE.

Joint	$\Delta_{CS}^{10}$	$\Delta_{FEE}$	MR
A	11.9	61.8	<b>79.7</b>
B	12.9	76.6	<b>96.0</b>
C	16.5	66.5	<b>91.2</b>
D	23.1	21.8	<b>56.5</b>
E	17.0	75.1	<b>100.6</b>
Abut.1	5.1	50.6	<b>58.2</b>

All values are expressed in centimeters

**Table 2:** Movement rating (MR) calculation for the expansion joints for the no-damper case.

Table 1 also shows the total seismic excursion values,  $\Delta_{SEE}$  for the SEE, which are defined as the difference between the maximum opening and minimum closing displacements. The maximum values among the three input ground motions (printed in bold) range between 33.6 to 117.9 cm, these two values corresponding to Joints D and B, respectively. In general, the excursion values are close to each other, except at Joint D where all three excursion values are considerably smaller than the corresponding values of the other locations. One reason for this result is the similarity of natural periods of vibration, and masses, of the frames on either side of Joint D. Because of this similarity, the frames tend to have synchronized motions at similar amplitudes and the joint relative displacements tend to be small. This observation is also in line with other numerical and experimental results on pounding between contiguous

structures where the relative velocity and the influence of pounding increase as the ratio between the frame periods departs from unity (Chau [4], DesRoches [11]).

Using the criteria expressed by Equation 1, the MR values can be determined by summing the creep and shrinkage components  $\Delta_{CS}^{10}$  with the seismic components  $\Delta_{FEE}$ . The values of the MR calculated using this criteria, together with the creep-shrinkage and seismic components for each location, are shown in Table 2. While the seismic components,  $\Delta_{FEE}$ , are derived directly from the safety level excursion values shown in Table 1 (i.e.  $\Delta_{FEE} = 65\% \Delta_{SEE}$ ), the values of  $\Delta_{CS}^{10}$ , shown in the second column of the table, were provided by CH2M HILL. The MR values for the structure without dampers range from 56.5 (Joint D) to 100.6 cm (Joint E), as shown in the last column of the table. These values represent the minimum displacements that the modular expansion joints need to accommodate without dampers and, therefore, they can be used to determine the minimum design size of the expansion joints. Note that although not directly shown here, the design values of initial gaps and the seat lengths at each of the joint locations are assumed to be sufficiently large to avoid pounding and joint unseating, respectively.

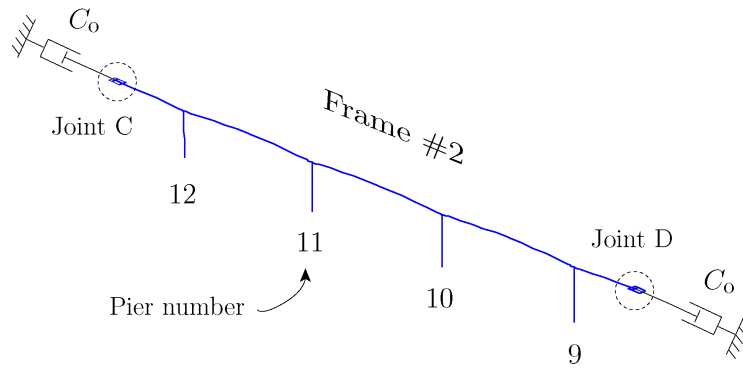


**Figure 2:** Model of Frame 2 isolated from the rest of the structure with linear FVDs at the two ends.

### PRELIMINARY DAMPER DESIGN

The goal of the preliminary analysis is the derivation of a set of dampers to be used as starting point for the non-linear time history analyses of the bridge model when FVDs are included. The approach consists of first determining damper sizes assuming that linear devices are used. Then, using a correlation based on an energy conservation approach, a corresponding set of non-linear devices are derived.

#### Linear damper size

The initial linear damper properties are obtained by considering the dynamic behavior of each frame isolated from the rest of the structure. Boundary conditions are imposed at the ends of the single frame so that the mutual effects of the adjacent frames can be approximated. First, the natural frequencies and mode shapes of the frames are determined using modal analyses. Then two dashpots, representing the combined effects of a set of linear viscous dampers, are introduced at the two ends of the model, as schematically shown in Figure 2. The two dashpots are considered to have the same properties. They are installed parallel to the longitudinal axis of the frame at the two joint locations to provide a more efficient configuration for the expansion joint size reduction. The damping coefficient  $C_o$  of the two dashpots can be obtained by using a method described by Constantinou [12] for the evaluation of the modal damping ratio of MDOF systems having additional damping. In general, the modal damping ratio  $\zeta_k$  corresponding to the  $k^{th}$  mode of a MDOF system can be written as (Chopra [13]):

$$\zeta_k = \frac{E_k}{4\pi S_k} \quad (2)$$

where  $E_k$  is the energy dissipated by the system during one sinusoidal cycle at the natural frequency,  $\omega_k$ , and  $S_k$  is the maximum value of the strain energy during the same cycle. For a system with supplemental damping, the modal damping ratio can be seen as the sum of the contribution of the internal system damping,  $\zeta_k^{(s)}$ , plus a contribution  $\Delta\zeta_k^{(d)}$  due to the supplemental damping devices (Constantinou [12]):

$$\zeta_k = \zeta_k^{(s)} + \Delta\zeta_k^{(d)} = \frac{E_k}{4\pi S_k} + \frac{D_k}{4\pi S_k} \quad (3)$$

where  $D_k$  is the total energy dissipated by the dampers. Using modal analysis, the values of the energy dissipated by the dampers,  $D_k$ , and the system strain energy,  $S_k$ , can be written as follows:

$$D_k = \pi\omega_k \Phi_k^T \mathbf{C}^{(d)} \Phi_k; \quad S_k = \frac{1}{2}\omega_k^2 \Phi_k^T \mathbf{M} \Phi_k \quad (4)$$

where  $\Phi_k$  is a column vector representing the  $k^{\text{th}}$  mode shape,  $\mathbf{C}^{(d)}$  is a matrix containing the damping coefficients of the supplemental devices and  $\mathbf{M}$  is the mass matrix of the system. In particular,  $\mathbf{C}^{(d)}$  is a diagonal matrix whose entries are the products  $C_j l_j^2$ ,  $C_j$  being the damping coefficient of the damper acting on the  $j^{\text{th}}$  degree of freedom and  $l_j$  the cosine of the angle formed by the damper and the direction associated with the  $j^{\text{th}}$  degree of freedom. Note that the diagonal entries of the  $\mathbf{C}^{(d)}$  assume a non-zero value only in the degrees of freedom where a damper acts (i.e. if no damper is associated with the  $j^{\text{th}}$  degree of freedom,  $C_j = l_j = 0$ ). Furthermore, if the modal vectors are normalized such that  $\Phi_k^T \mathbf{M} \Phi_k = 1$ , this matrix product disappears on the expression of  $S_k$  in Equation 4. Therefore, the increment of the modal-damping ratio due to supplemental damping devices can be written as follows:

$$\Delta\zeta_k^{(d)} = \frac{1}{2\omega_k} \sum_{i=1}^n C_i l_i^2 \phi_i^2 \quad (5)$$

where the matrix product  $\Phi_k^T \mathbf{C}^{(d)} \Phi_k$  is explicitly written as a summation over the total number of degrees of freedom  $n$ , and  $\phi_i$  is the  $i^{\text{th}}$  component of the modal vector,  $\Phi_k$ . If we assume that the dampers are the same in all locations, as for the case of our bridge frame models, the common damping coefficient value,  $C_o$ , can be extracted from the summation and calculated as follows:

$$C_o = 2\omega_k \frac{\Delta\zeta_k^{(d)}}{\sum_{i=1}^n l_i^2 \phi_i^2} \quad (6)$$

Therefore, for a given target value of the modal damping ratio, the damping coefficient  $C_o$  can be calculated using the modal analysis results.

Considering the case of Frame #2 shown in Figure 2, the modal analysis shows that the mode that produces larger deformations in the longitudinal degrees of freedom at the joint locations is mode #4. Only two dampers are installed and they are acting along the displacement degrees of freedom #32 and #548, respectively. The modal analysis provides the following data:  $T_4=2.4604$  sec ( $\omega_4=2.554$  rad/sec),  $\phi_{32}=0.04850$  and  $\phi_{548}=0.04986$ . Note that  $l_{32}=l_{548}=1$ , since both dampers are aligned with the corresponding degrees of freedom. Using these values and assuming a target incremental modal damping ratio  $\Delta\zeta_k^{(d)}=15\%$ , the damping coefficient for Frame #2 is  $C_o=158.34$  kN sec/cm. Note that  $\Delta\zeta_k^{(d)}=15\%$  was chosen so that the total modal damping ratio is increased to 20% (assuming the internal structure damping ratio  $\Delta\zeta_k^{(s)}=5\%$  for a concrete structure designed to experience only minor, repairable damage). The values of the frequencies and damping coefficients for the four frames of the bridge are shown in Table 3.

Frame #	$\omega_k$ (rad/sec)	$C_o$ (kN sec/cm)
1	2.96	185.55
2	2.55	158.34
3	2.43	370.09
4	1.85	50.04

**Table 3:** Preliminary values of damping coefficients for linear FVDs.

Equations 2 and 3 are based on the assumption that the free-vibration natural frequencies of the damped system are the same as those of the undamped system. Due to the high value of supplemental damping introduced by the dampers, this assumption is not strictly valid for the model considered (Chopra[13]). However, comparisons of experimental results with theory have shown that Equation 3 is sufficiently accurate even when relatively high values of supplemental damping are introduced in the system (Constantinou [12]).

### Correlation between linear and non-linear FVDs

Fluid viscous dampers (FVDs) are passive devices that have been used often in retrofit applications of major bridges, as well as in a few new structures. These devices show viscoelastic behavior for a wide range of frequencies of the input excitation. In general, the response of a FVD is controlled by its geometric features, in particular the size and shape of the orifices of the piston head, and by the viscous properties of the fluid (Symans [14]). The response of seismic viscous dampers can be expressed by the following fractional velocity power law:

$$F_D = C_\alpha \operatorname{sgn}(\dot{u}) |\dot{u}|^\alpha \quad (7)$$

where  $F_D$  is the force developed by the device,  $C_\alpha$  is the damping coefficient,  $\operatorname{sgn}()$  is the signum function,  $\dot{u}$  is the piston velocity with respect to the damper housing, and the exponent  $\alpha$  is a real number that generally ranges between 0.2 and 1.0, as specified for a given application. If the device is subjected to a sinusoidal input  $u = u_o \sin(\omega t)$ , the energy dissipated by the FVD during one cycle of the harmonic motion is:

$$E_D = \pi \beta_\alpha C_\alpha \omega^\alpha u_o^{1+\alpha} \quad (8)$$

where  $\omega$  is the input angular velocity,  $u_o$  the peak displacement and  $\beta_\alpha$  a parameter that depends on the exponent  $\alpha$  (Symans [14]). Note that Equations 7 and 8 are general expressions and can be used to represent many damper responses, such as those of friction dampers ( $\alpha=0$ ), linear viscous dampers ( $\alpha=1$ ), and non-linear viscous dampers for all the values of  $\alpha$  between zero and one.

Non-linear FVDs are suitable for applications where large forces and velocities are expected, such as in bridge applications (Symans [14]). The exponent of the velocity of the devices used for the analyses presented in this paper, is chosen to be  $\alpha=0.2$ . This value is believed to represent the lowest value that can be currently manufactured at a reasonable price. Dampers with lower  $\alpha$  's are available but the additional cost is prohibitive versus the increase in performance and energy absorption. Energy considerations are used here to relate linear and non-linear FVDs. For the purposes of sizing nonlinear FVDs, a non-linear FVD is considered to be "equivalent" to a linear FVD, if both devices dissipate the same amount of energy while subjected to the same series of input motions. Because it is not possible to find two devices that satisfy this requirement for all inputs, we restrict our definition to a series of sinusoidal motions at a specified frequency. Since the frame fundamental frequency chosen for each frame (Table 3) is the frequency component that is more likely to produce larger deformations at the damper locations, this frequency is chosen as the frequency of the input motions for this equivalence criteria. Furthermore, for

the chosen frequency, the maximum amplitude  $u_o$  is swept from 0 to a target value  $u_o^*$ . This criteria can be mathematically expressed as follows:

$$\int_0^{u_o^*} E_{D(\alpha=1)} du_o = \int_0^{u_o^*} E_D du_o \quad (9)$$

where  $E_{D(\alpha=1)}$  represents the energy dissipated by a linear FVD. Substituting the energy values and moving the constant values outside the integrals, we obtain:

$$\pi C_o \omega \int_0^{u_o^*} u_o^2 du_o = \pi \beta_\alpha C_\alpha \omega^\alpha \int_0^{u_o^*} u_o^{1+\alpha} du_o \quad (10)$$

After solving the integrals, the value of  $C_\alpha$  can be expressed as follows:

$$C_\alpha = C_o(2 + \alpha) \frac{\omega^{(1-\alpha)} u_o^{*(1-\alpha)}}{3\beta_\alpha} \quad (11)$$

Note that when  $\alpha=1$ , then  $\beta_\alpha=1$  and Equation 11 becomes  $C_\alpha=C_o$ . Using Equation 11, it is possible to derive the damping coefficient  $C_\alpha$  from the  $C_o$  values of each of the four frames of the bridge. All the parameters necessary to calculate the damping coefficients are available except for the maximum target displacement,  $u_o^*$ . However,  $u_o^*$  can be determined by using the results of the time history analysis of the structure without dampers, considering that the expected (and targeted) displacement reduction due to the introduction of dampers is on the order of 30-40%. For each frame, an average value of the maximum excursions due to the safety level earthquake loadings (Table 1) is calculated. Then  $u_o^*$  is set to be 70% (i.e. 30% reduction) of half of these average values. The target amplitude  $u_o^*$ , together with the calculated damping coefficients of the set of non-linear dampers, are shown in Table 4.

Frame	Frequency (rad/sec)	$C_o$ (linear)		$C_\alpha$
		$\alpha = 1.0$ (kN sec/cm)	$u_o^*$ cm	$\alpha = 0.2$ (kN sec <sup>0.2</sup> /cm <sup>0.2</sup> )
#1	$\omega = 2.96$	185.55	31	4209.1
#2	$\omega = 2.55$	158.34	21	2334.9
#3	$\omega = 2.43$	370.09	22	5449.3
#4	$\omega = 1.85$	50.04	29	738.9

**Table 4:** Damper coefficients of equivalent linear and non-linear dampers.

The equivalent criteria is graphically represented in Fig 4a, for the case of Frame #1. In the figure, the hysteretic energy values for both linear and non-linear devices are plotted as function of the max amplitude  $u_o$ . The criteria expressed by Equation 9 simply imposes the equivalence of the areas underneath the two curves. In Fig. 4b, the two hysteretic loops for the dampers are plotted for the case in which  $u_o$  is equal to the target maximum amplitude  $u_o^*=31$  cm.

Each of the damper coefficients shown in Table 4 is related to one frame. However, each intermediate joint corresponds to two contiguous frames and the value of the initial damping coefficients need to be defined at each joint. At this point of the analysis, the values of the coefficient at the intermediate joint are determined as the average between the two frame values. Table 5 shows the initial non-linear damper coefficients assigned at each joint location. We will follow with some comments on the selection of these initial values in the next section and in the final conclusions, after the some results of the time history analysis have been presented.

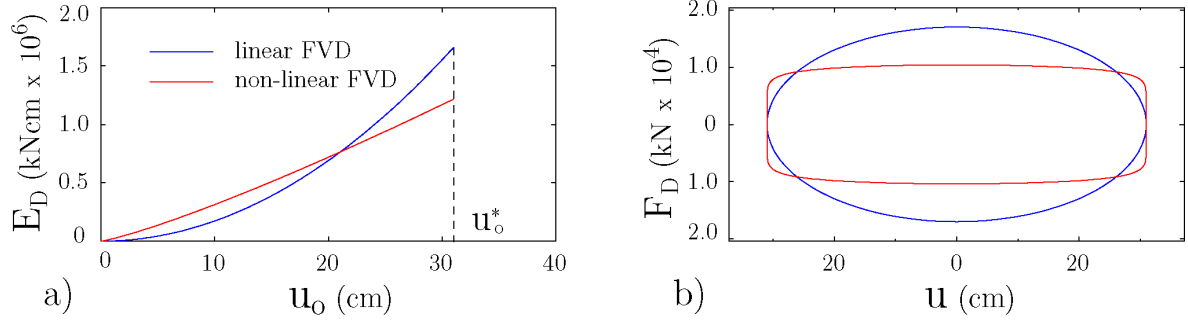


**Figure 3:** Equivalent linear and non-linear FVDs. a) Hysteretic energy values vs maximum amplitude and b) damper hysteretic loops at  $u_o = u_o^*$ .

### NON-LINEAR TIME HISTORY ANALYSIS (WITH DAMPERS)

Using the initial set of damping coefficients, several analyses were performed considering different combinations of damper installations. For example, dampers were considered in Joint A but not in the other locations. Next, dampers were considered only in Joint B, and so on, until all relevant combinations were examined. Each configuration was subjected to all three input ground motions. The effects of the successive introduction of dampers in the structure were constantly monitored at all the locations of interest, including the joints or abutment in which dampers were not to be installed (i.e. North approaches). This process was possible because of the relative short time necessary to run a single analysis (about 10 minutes). The reductions of the relative displacements at the joint locations were all close to the target values assumed at the beginning of the analysis. These results confirmed that the approach used in the preliminary analysis was able to provide reasonable size of the non-linear dampers.

Joint	$C_\alpha^{(1)}$ ( $\text{kN sec}^{0.2}/\text{cm}^{0.2}$ )	$C_\alpha^{(2)}$ ( $\text{kN sec}^{0.2}/\text{cm}^{0.2}$ )
A	2104.5	1700
B	2104.5	1700
C	3272.0	3400
D	3892.1	3400
E	3094.1	3400
Abut.1	738.9	2300

(1) Preliminary analysis values

(2) Refined values

**Table 5:** Refined values of the preliminary damper coefficients at all joint locations.

After checking the initial damping coefficients, a process of refining these values was started by modifying each damper set at a time and running the analysis for the three ground motions. The joint displacements at all joint locations were constantly monitored and compared. The refined values of the damping coefficients are shown in the last column of Table 5, next to the values of the preliminary analysis. These refined values have been rounded and adjusted so that they correspond to a certain number of commercially available seismic non-linear FVDs. Except for the case of Abutment 1, the refined values are close to the preliminary values. The large difference at the abutment location can be partially explained by the difference in fundamental periods and masses of Frame #4 and the other major frames. While the period of Frame #4 is about 3.4 sec, the period of Frame #3 (the contiguous frame) is about 2.6 sec and the ratio between the masses is about 1/5. The major assumption of the preliminary analysis was to consider each frame isolated from the rest of the structure. By doing so, the mutual interactions between

the frames are neglected. While this assumption is reasonable for contiguous frames having similar periods and masses (i.e. the contiguous frames are able to provide sufficiently strong inertial reactions to each other) this is not true when the differences are large.

Dampers		Ground motion #1			Ground motion #2			Ground motion #3		
Joint	$C_\alpha$	Max open.	Min closing	Total displ.	Max open.	Min closing	Total displ.	Max open.	Min closing	Total displ.
A	1700	10.9	-12.6	<b>23.5</b>	6.8	-6.0	12.8	10.6	-9.6	20.2
B	1700	21.7	-13.7	35.4	15.2	-10.9	26.1	22.8	-20.5	<b>43.4</b>
C	3400	12.6	-15.2	27.8	12.7	-12.6	25.4	15.9	-16.8	<b>32.7</b>
D	3400	4.2	-5.0	9.2	3.9	-4.3	8.2	5.5	-8.8	<b>14.3</b>
E	3400	13.9	-9.4	<b>23.3</b>	6.9	-5.4	12.3	10.3	-9.1	19.4
Abut.1	2300	18.6	-13.5	<b>32.1</b>	15.1	-15.7	30.8	15.9	-15.4	31.3

Displacements expressed in centimeters - Damping coefficients in  $\text{kN sec}^{0.2}/\text{cm}^{0.2}$

**Table 6:** Opening and closing displacements at the joint locations for the model with dampers subjected to the three input ground motions at FEE.

Dampers		Ground motion #1			Ground motion #2			Ground motion #3		
Joint	$C_\alpha$	Max open.	Min closing	Total displ.	Max open.	Min closing	Total displ.	Max open.	Min closing	Total displ.
A	1700	24.5	-24.6	<b>49.1</b>	17.3	-15.9	33.2	21.0	-21.2	42.3
B	1700	39.1	-26.1	65.2	27.9	-22.4	50.4	41.0	-36.7	<b>77.7</b>
C	3400	23.6	-26.3	49.9	23.4	-23.3	46.7	28.7	-29.1	<b>57.8</b>
D	3400	7.2	-8.5	15.7	5.9	-7.5	13.4	9.8	-13.5	<b>23.3</b>
E	3400	25.8	-23.1	<b>48.9</b>	16.6	-14.4	31.0	21.4	-17.6	39.0
Abut.1	2300	29.0	-22.8	<b>51.8</b>	25.5	-23.0	48.5	24.0	-23.2	47.2

Displacements expressed in centimeters - Damping coefficients in  $\text{kN sec}^{0.2}/\text{cm}^{0.2}$

**Table 7:** Opening and closing displacements at the joint locations for the model with dampers subjected to the three input ground motions at SEE.

The joint relative displacements from the non-linear time history analysis are shown in Tables 6 and 7 for the FEE and SEE level events, respectively. As with the non-damper case, the total relative displacements (i.e. joint excursions) are calculated as the difference between the maximum opening and the minimum closing during the duration of each input motion. The values in bold represent the maximum relative displacements among all three input cases. Comparing these values with the corresponding maximum values for the case without dampers (Table 1), it is clear that the introduction of dampers significantly reduces the relative displacements between the frames. Without dampers, the maximum excursions range from 33.6 to 117.9 cm; when the selected dampers are used, the corresponding values range from 23.3 to 77.7 cm (SEE level ground motion). The plot of the opening/closing relative displacement as function of time for Set #2 of the SEE motion at the Joint C is shown in Figure 4a. Figure 4b shows the total force-displacement loops of the dampers at Joint C for the same input motion but for the SEE case.

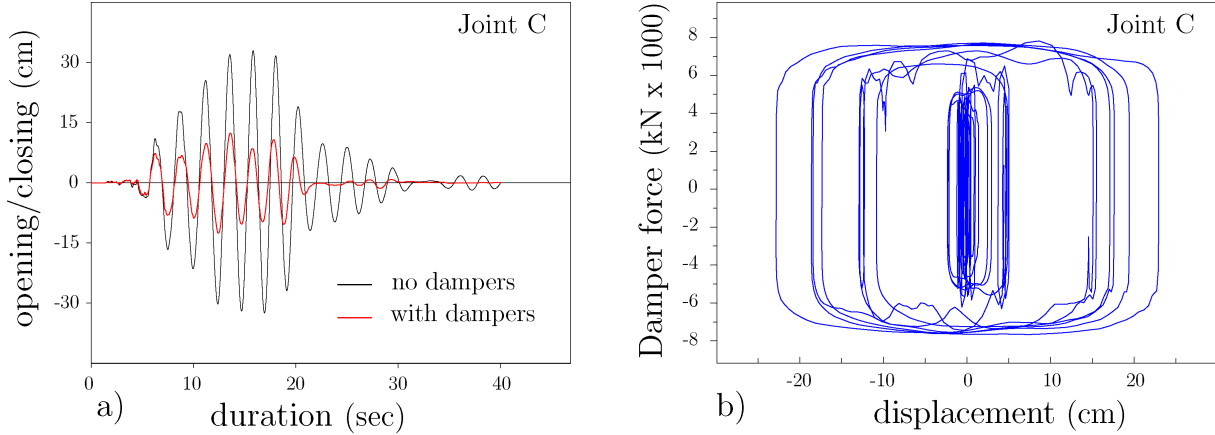


**Figure 4:** Response at Joint C. a) Opening/closing vs time comparison for the cases with and without dampers (FEE input), and b) damper force vs displacement (SEE input).

One important effect of the introduction of the energy dissipation devices in the structure is the reduction of the opening and closing displacements at the joint locations. As discussed in a previous section, one of the components of the movement rating of the expansion joint is the seismic deformation,  $\Delta_{FEE}$ , defined as the maximum relative joint displacement due to the functional level input motions. By comparing the maximum excursions values of the cases with and without dampers for the functional level case, we can see that the reductions ranges between 42 to 75 % with an average value of 54 %. Therefore, we can expect a considerable reduction of the size and, therefore, cost of the expansion joints (Equation 1). Table 8 summarizes the MR values obtained with and without the nonlinear FVDs. Because of the importance of the seismic component in the MR calculation, the size reductions of the joints are large, ranging from 13.3 to 51.5 % with respect to the original size. On average, for the case considered in this study, the expansion joint size can be reduced by 36% when installed in conjunction with FVDs. The importance of this is that the cost of introducing dampers into the system is often more than paid for by the reduction in cost of the expansion joints when the joints include seismic component in their sizing. Another side benefit is the reduction in longitudinal displacement of the piers, possibly resulting in additional cost savings.

Joint	$\Delta_{CS}^{10}$	$\Delta_{FEE}$	MR (dampers)	MR (no d.) (no dampers)	Reduc.(%)
A	11.9	23.8	<b>41.7</b>	79.7	47.6
B	12.9	43.4	<b>62.7</b>	96.0	34.6
C	16.5	32.7	<b>57.4</b>	91.2	37.1
D	23.1	14.3	<b>48.5</b>	56.5	13.3
E	17.0	23.3	<b>48.8</b>	100.6	51.5
Abut.1	5.1	32.1	<b>39.7</b>	58.2	31.8

Displacements expressed in centimeters

**Table 8:** Movement rating (MR) of the expansion joints

## CONCLUSIONS

The effects of passive dissipation devices, such as fluid viscous dampers, on bridge deck expansion joints have been investigated through a numerical example. Because of the high-energy dissipation capacity of the FVDs, the seismic response of a bridge can be substantially improved when these devices are used. In particular, the seismic relative displacements at joint locations can be reduced. For the bridge structure and input motions considered in this paper, the size of the modular expansion joints can be reduced up to

51.5% with respect to the original design size (no-damper case). The introduction of dampers into the model also reduces the relative velocities between adjacent bridge frames. Smaller velocities imply smaller impact forces, and potentially less damage, if contact occurs between adjacent frames or between components of expansion joints.

A simple method to estimate appropriate non-linear damper coefficients is presented in the first part of the paper. The method involves analyzing each frame independently, with linear FVDs inserted between the frame and fixed points; energy dissipation concepts are used to determine the nonlinear FVD coefficients from the linear FVD coefficients and the target relative displacements at the joints. Non-linear time history analyses of the bridge system indicated that these preliminary estimates of the damper coefficients are sufficiently accurate for most of the joints considered. When the natural periods and/or masses of adjacent frames are quite different, however, this method is limited in that the mutual effects of interaction between adjacent frames are not included. Averaging the damper coefficient values associated with the two frames defining each joint is not sufficient in such cases, including the joints associated with Frame # 4 in the example. The simplified method needs to be improved so that frame interaction effects, which generally become pronounced when there are differences in natural period and/or mass between adjacent frames, are taken into account more accurately.

Throughout the numerical analyses, the model was considered to remain linear elastic. This assumption is valid because the structure, in this example, has been designed to remain mostly elastic for all the loading conditions even without dampers. However, in this study the local effects of the concentrated forces developed by the dampers have not been considered, nor have the damper force effects on the foundations (e.g. Abutment 1). This set of forces can be large and they would need to be included in the final design of the structure. Also, non-uniform excitation of the model supports was not considered in this work. For large bridges, the supports are relatively far apart and can be excited by different motions that are not acting simultaneously. This effect can be very important and the dynamic response of the structure can be very different from the case in which all the supports are excited by the same input simultaneously. Although further research needs to be done, the results from this study show that passive devices can provide an effective solution to mitigate bridge seismic responses and, at the same time, reduce the size and cost of modular expansion joints. Designing modular expansion joints to accept large seismic displacements (both opening and closing) and maintaining functionality at expected speeds of movement is also a challenge that the joint industry is just beginning to tackle [15].

## ACKNOWLEDGEMENTS

This study has been supported by CH2M HILL, Inc. The authors would like to express their gratitude to CH2M HILL for the technical support and for providing the finite element models used for the analyses.

## REFERENCES

1. Roeder, CW. "Fatigue and dynamic load measurements on modular expansion joints." *Construction and Building Materials* 1998; Elsevier Science Ltd; 12(2-3): 143-50.
2. Chang L, Lee Y. "Evaluation of performance of bridge deck expansion joints." *Journal of Performance of Constructed Facilities* 2002; ASCE; 16(1): 3-9.
3. Malhotra PK. "Dynamics of seismic pounding at expansion joints of concrete bridges." *Journal of Engineering Mechanics* 1998; ASCE; 124(7): 794-802.
4. Chau KT, Wei XX, Guo X, Shen CY. "Experimental and theoretical simulations of seismic pounding between two adjacent structures". *Earthquake Engineerings and Structural Dynamics* 2003; 32: 537-54.

5. Trochalachis P, Eberhard MO, Ricles J. "Design of seismic restrainers for in-span bridges." *Journal of Structural Engineering* 1997; ASCE; 123(4): 469-78.
6. DesRoches R, Fenves GL. "Design of seismic cable hinge restrainers for bridges." *Journal of Structural Engineering* 2000; ASCE; 126(4): 500-9.
7. Moehle JP. "Northridge earthquake of January 17, 1994: Reconnaissance report, Highway bridges and traffic management." *Earthquake Spectra* 1995; 11(S2): 287-372.
8. Feng MQ, Kim J, Shinozuka M, Purasinghe R. "Viscoelastic dampers at expansion joints for seismic protection of bridges." *Journal of Bridge Engineering* 2000; ASCE; 5(1): 67-74.
9. Strandgaard H, "Design and application of energy dissipating dampers on a new concrete bridge in California." 7th International Symposium on Smart Structures and Materials-Damping and Isolation, Newport Beach, CA, March 2000.
10. Wilson, E.L. "Three Dimensional Static and Dynamic Analysis of Structures." *Computers & Structures Inc., Berkeley, CA, 1998.*
11. DesRoches R, Muthakumar S. "Effect of pounding and restrainers on seismic response of multiple-frame bridges." *Journal of Structural Engineering* 2002; ASCE; 128(7): 860-69.
12. Constantinou MC, Symans MD. "Experimental and Analytical Investigation of Seismic Response of Structures with supplemental Fluid Viscous Dampers." Technical Report NCEER-92-0032, NCEER, SUNY/Buffalo, 1992.
13. Chopra AK. "Dynamics of Structures - Theory and Applications to Earthquake Engineering." Prentice Hall, Upper Saddle River, NJ, 1995.
14. Symans MD, Constantinou MC. "Passive fluid viscous damping systems for seismic energy dissipation." *ISET Journal of Earthquake Technology* 1998; 35(4): 185-206.
15. Clyde D. "Full-scale Dynamic Testing of Expansion Joints for Seismically Isolated Bridges." Technical Report EERCL 2002-01, PEERC, University of California, Berkeley, 2002.